LETTERS TO THE EDITOR

The Letters to the Editor section is divided into four categories entitled Communications, Notes, Comments, and Errata. Communications are limited to three and one half journal pages, and Notes, Comments, and Errata are limited to one and three-fourths journal pages as described in the Announcement in the 1 January 1997 issue.

COMMUNICATIONS

Competition between singlet and triplet channels in the photoinitiated decomposition of HNCO

M. Zyrianov, Th. Droz-Georget, and H. Reisler
Department of Chemistry, University of Southern California, Los Angeles, California 90089-0482

(Received 7 February 1997; accepted 27 February 1997)

The spin-forbidden channel, NH($X\ ^3\Sigma^-$)+CO, has been observed directly in the photodissociation of jet-cooled HNCO following $S_1 \leftarrow S_0$ excitation. The NH($X\ ^3\Sigma^-$) yield spectrum is obtained in the energy regimes near the thresholds to H+NCO and NH($a\ ^1\Delta$)+CO channels. The spectrum is similar to the NCO yield spectrum when direct dissociation on S_1 is not significant. At photolysis energies $>43\,400$ cm^{-1}, state specific differences between the NH($X\ ^3\Sigma^-$), NH($a\ ^1\Delta$) and NCO yield spectra are observed, and at energies $>44\,000$ cm^{-1} all structure in the NH($X\ ^3\Sigma^-$) yield spectrum is lost, while the NH($a\ ^1\Delta$) yield spectrum remains structured. The results are interpreted in terms of the different time scales for intersystem crossing and dissociation. © *1997 American Institute of Physics.* [S0021-9606(97)04917-9]

I. INTRODUCTION

The photoinitiated decomposition of HNCO following excitation to the first excited singlet state $S_1(^1A'')$ can terminate in three channels: (1) ^{3}NH+CO, (2) H+NCO, and (3) ^{1}NH+CO [^{3}NH and ^{1}NH denote NH($X\ ^3\Sigma^-$) and NH($a\ ^1\Delta$), respectively]; and involve at least three potential energy surfaces (PESs): $S_1(^1A'')$, $T_1(^3A'')$, and $S_0(^1A')$.[1–13] Although dissociation on S_1 can occur as soon as the photolysis energy exceeds D_0(H+NCO)=38 370 cm^{-1},[8(b),9] recent results indicate the existence of barriers to direct S_1 decomposition, and therefore near D_0(H+NCO) the preferred route is predissociation on S_0 following radiationless decay.[7,9] Just above the threshold to channel (3) [$D_0(^1\text{NH}+\text{CO})=42\,765$ cm^{-1}],[10] predissociation on S_0 is still suggested, but dissociation on S_1 to ^{1}NH+CO starts to play a larger role at higher photolysis energies.[8,10] The participation of triplet surfaces accessed by intersystem crossing (ISC) has not been investigated in detail; indirect evidence that at 248 nm the ^{3}NH+CO channel, which correlates with T_1, constitutes ~0.05 of the total yield was obtained in photolysis of 300 K HNCO.[11]

This Communication reports results obtained by direct observation of the ^{3}NH+CO channel. We concentrate on dissociation in the energy regimes near the thresholds to H+NCO and ^{1}NH+CO. In the former region, channels (1) and (2) evolve via radiationless decay; in the latter region all three channels are observed simultaneously, and direct S_1 dissociation becomes important.[7–10] In addition, Brown *et al.* have shown that in this region the branching ratio between H+NCO and ^{1}NH+CO changes when implanting NH stretch excitation in HNCO(S_0) prior to photodissociation.[7] Our results show that dissociation via T_1 is significant in both energy regimes and that ^{3}NH can be detected even at photolysis wavelengths where dissociation on S_1 is dominant. The most intriguing result is the observation of a selective loss of structure in the ^{3}NH yield spectrum at photolysis wavelengths where the ^{1}NH yield spectrum still exhibits distinct structural features. In order to rationalize this observation we propose that the ^{3}NH and ^{1}NH yield spectra monitor different time scales.

II. EXPERIMENT

The experimental arrangement and conditions used in these pump-probe experiments were described previously.[9,14] ^{3}NH products from jet-cooled HNCO were probed under non-saturated conditions by laser induced fluorescence (LIF) via the $A\ ^3\Pi \leftarrow X\ ^3\Sigma^-$ transition,[15] using an excimer laser pumped dye laser (pulse energy ~7–120 μJ in 2–3 mm diam beam). For relative branching ratio measurements, a broadband glass filter (Kopp 0–56) was used in the detection system to ensure flat spectral response in the wavelength region of interest. The recorded spectra were corrected for scattered light and laser intensity variations. The linear dependence of the ^{3}NH signal on laser power ensured that it derived from one-photon dissociation of HNCO. The ^{1}NH and NCO($X\ ^2\Pi$) yield spectra were obtained as described elsewhere.[9]

III. RESULTS

Figure 1 presents ^{3}NH [trace (a)] and NCO [trace (b)], yield spectra in the region of the channel (2) threshold. The spectra are not normalized to either the absorption coefficient or the fractional population of the monitored levels, and thus do not reflect the correct branching ratios. Both spectra have similar structure, and no significant changes are observed in the ^{3}NH yield as the excitation energy exceeds

 0021-9606/97/106(17)/7454/4/$10.00

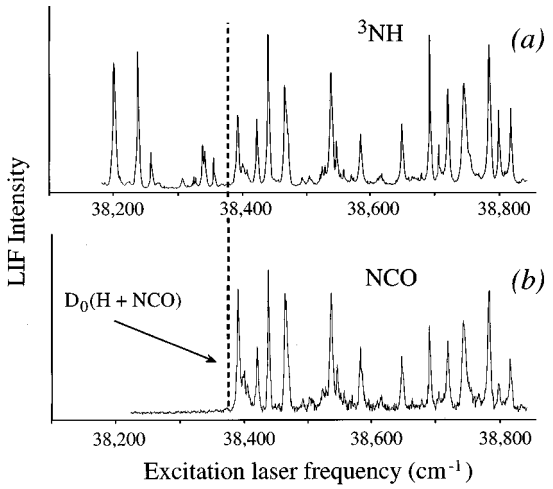

FIG. 1. Photofragment yield spectra obtained in HNCO decomposition via channels (1) and (2) near the threshold to H+NCO. The traces were obtained by monitoring (a) the Q bandhead of the NH ($A\ ^3\Pi \leftarrow X\ ^3\Sigma^-$) transition and (b) the Q_{11} bandhead of the NCO $A\ ^2\Sigma^+ \leftarrow X\ ^2\Pi$ (00^00-00^10) transition. The vertical dashed line indicates D_0(H+NCO).

D_0(H+NCO). From the S_1 origin ($\leqslant$35 000 cm^{-1})[13] onward, the ^{3}NH yield spectrum is nearly identical to the HNCO two-photon excitation spectrum reported earlier.[9] State-specificity in linewidths is observed both in the two-photon excitation spectrum and in the ^{3}NH yield spectra, and representative examples of C-type vibronic bands are shown in Fig. 2. While some bands exhibit well pronounced rotational structure, others show virtually no structure.

Figure 3 presents NCO, ^{3}NH, and ^{1}NH yield spectra [traces (a), (b), and (c) respectively] in the region of the threshold to channel (3). As in Fig. 1, the relative intensities within each spectrum are correct; however, the three traces are not normalized to reflect the relative branching ratios of channels (1)–(3), nor to the total absorption cross-section, which increases sharply in this region.[1] The observed decrease in the ^{1}NH intensity above ~44 500 cm^{-1} does not signify a drop in its quantum yield, but rather is due to a decrease in the monitored ^{1}NH($J=2$) fractional population with excitation energy.[9] Neither the ^{3}NH nor the NCO yield spectra exhibit significant changes in intensities and widths of spectral features when the dissociation threshold to channel (3) is crossed. Three regimes of photolysis energy can be distinguished: (i) up to ~43 400 cm^{-1} (230 nm), nearly identical and well pronounced structure is observed in all three spectra; (ii) between ~43 400 cm^{-1} (230 nm) and ~44 000 cm^{-1} (227 nm) several features that are clearly observed in the ^{1}NH yield spectrum (c) are missing in the ^{3}NH spectrum (b), and sometimes in the NCO spectrum (a), as highlighted by vertical solid lines in Fig. 3; and (iii) at photolysis energies exceeding ~44 000 cm^{-1} (227 nm) all sharp features in the ^{3}NH yield trace disappear and the spectrum exhibits only residual broad features on top of a background. On the other hand, the yield spectra recorded for channels (2) and (3) remain fairly structured.

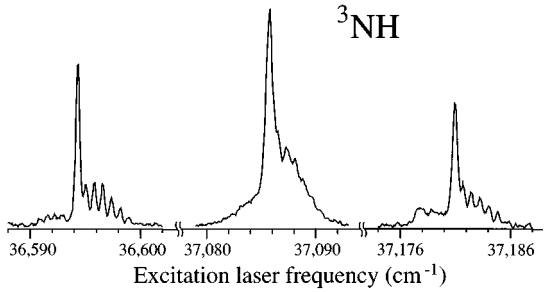

FIG. 2. Rotational contours of selected C-type bands in the ^{3}NH photofragment yield spectrum below the H+NCO channel threshold. The Q bandhead of the NH ($A\ ^3\Pi \leftarrow X\ ^3\Sigma^-$) transition was monitored.

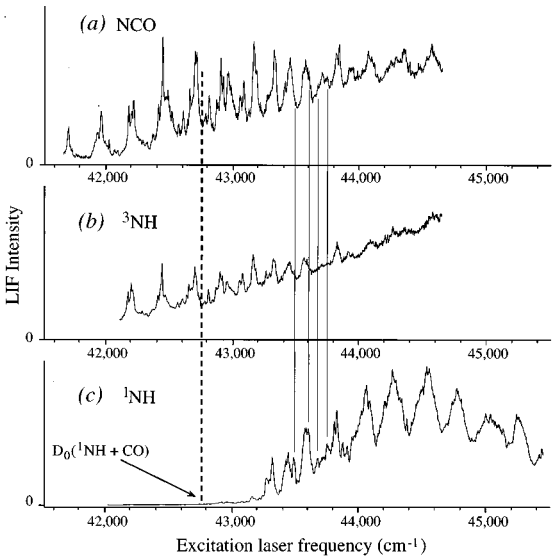

FIG. 3. Photofragment yield spectra obtained in HNCO decomposition via channels (1)–(3) near the threshold to ^{1}NH+CO. The traces were obtained by monitoring (a) the Q_{11} bandhead of the NCO $A\ ^2\Sigma^+ \leftarrow X\ ^2\Pi$ (01^10-01^20) transition; (b) the Q bandhead of the NH($A\ ^3\Pi \leftarrow X\ ^3\Sigma^-$) transition; (c) the $Q(2)$ line of the NH($c^1\Pi \leftarrow a^1\Delta$) transition. The vertical dashed line indicates D_0(^{1}NH+CO); solid lines highlight positions at which state-specificity is observed in the spectra (see the text for details).

^{1}NH/^{3}NH population ratios were obtained at 230, 225.2, and at 224.5 nm. The ratio at 230 nm was obtained in two ways. In method (i) rotational populations of ^{1}NH and ^{3}NH were determined and corrected by normalization factors as described elsewhere.[14] In method (ii), the integrated intensities of the rotational branches in the LIF spectra were normalized as per their relative weights in the electronic transitions. The ^{1}NH/^{3}NH population ratio was then determined from the ratio of the integrated intensities of all the branches after applying the same corrections as in method (i). Although the second approach is less accurate, both methods gave results that agree within 25% at 230 nm, and therefore only the second approach was used at ~225 nm. The ^{1}NH/^{3}NH population ratios were 0.2 at 230 nm (43 480 cm^{-1}), 1.7 at 225.2 nm (44 405 cm^{-1}), and 2.1 at 224.5 nm (44 540 cm^{-1}). Note that 224.5 nm corresponds to a peak in the ^{1}NH yield spectrum while 225.2 nm corresponds to a valley (Fig. 3). The uncertainty in the absolute population ratios is determined primarily by the normalization factors

and is estimated at 30%, while the relative precision of these measurements is 10%.

IV. DISCUSSION

The most intriguing aspect of the results reported here is the progressive loss of structure in the ^{3}NH yield spectrum shown in Fig. 3. This loss of structure is accompanied initially by state-specificity; several peaks in the ^{1}NH spectrum are missing or diminished in intensity in the ^{3}NH spectrum, and to a lesser extent in the NCO spectrum. The latter spectrum, in fact, has an appearance intermediate between those of ^{3}NH and ^{1}NH. In order to understand these observations we first briefly discuss the decomposition mechanism at lower energies in view of what is currently known about the participating PESs.

The S_1 equilibrium geometry, inferred from spectroscopic data[1] and supported by several calculations,[8,13,16] is planar with an NCO angle of $\sim$120° (172° on S_0), and an HNC angle of $\sim$110°. Upon $S_1 \leftarrow S_0$ excitation the N–C bond extends from 1.214 Å to 1.35 Å, indicating a decrease in bond order. Thus, S_1 is expected to be repulsive along the N–C coordinate in the Franck–Condon (FC) region. Recent calculations show that T_1, whose origin lies $\sim$1800 cm^{-1} below the ^{3}NH+CO asymptote, has a non-planar equilibrium geometry with an NCO angle and N–C bond length similar to those in planar HNCO(S_1). Also, exit barriers of $\sim$3200 cm^{-1} and $\sim$1800 cm^{-1} to the H+NCO and ^{3}NH+CO asymptotes, respectively, have been calculated.[12] Preliminary calculations using the Gaussian 94 package at the CIS/6-311++G(3df,3pd) level show that a second triplet state, $T_2(A')$, which is also nonplanar, lies close to $T_1(A'')$ in the FC region.[13]

Previous experimental investigations of the spin-allowed photodissociation pathways following $S_1 \leftarrow S_0$ excitation up to and slightly above the threshold to ^{1}NH+CO inferred a mechanism involving internal conversion (IC) followed by predissociation on S_0 without notable barriers to channels (2) and (3).[7,9,10] This implies significant barriers on S_1, in accordance with recent 3D calculations that estimate barriers on S_1 in both the H+NCO and ^{1}NH+CO channels of the order of 6000-8000 cm^{-1} and $<$1000 cm^{-1}, respectively.[17] Thus, only at energies $\sim$1000 cm^{-1} above $D_0(^1\text{NH+CO})$, S_1 dissociation to channel (3) is expected to be important. The onset of S_1 dissociation to channel (2) may be even higher, despite the 4400 cm^{-1} difference in the dissociation thresholds to these two channels.

The spin-forbidden pathway, channel (1), must proceed on T_1. The similar appearance of the ^{3}NH and NCO yield spectra in Fig. 1, the similarity between the ^{3}NH yield and two-photon excitation spectra from the S_1 origin ($<$35 000 cm^{-1}) onward, and the successful assignment of this spectrum to the $S_1 \leftarrow S_0$ transition,[13] show that the formation of ^{3}NH at these photolysis energies involves ISC to T_1 rather than direct $T_1 \leftarrow S_0$ excitation. Since all excitation energies accessible via S_1 are $>$5000 cm^{-1} above the channel (1) threshold, the ^{3}NH+CO dissociation involves the repulsive part of T_1 with fast and direct formation of products. The distinct structural features in the ^{3}NH yield spectrum must be therefore related to the radiationless decay time scales. Above D_0(H+NCO) the width of the spectral features and the intensity of the structureless background increase gradually with photolysis energy in a similar fashion to that observed for the NCO yield spectrum, supporting the conclusion that as long as the ^{1}NH+CO pathway is not accessible directly on S_1, the only routes leading to dissociation involve radiationless decay.

In C_s symmetry $S_1(^1A'')$ and $T_1(^3A'')$, which have the same electronic configuration, may be coupled both directly and via an intermediate state, e.g., S_0 and/or another triplet state. The couplings among electronic states depend not only on the spin-orbit electronic coupling matrix elements, but also on vibrational overlap FC factors, i.e., on the topology of the multidimensional PESs involved. This clearly manifests itself in the state-specificity observed in the rotational contours of the ^{3}NH yield spectrum (Fig. 2), demonstrating that the ISC step depends sensitively on the level excited in S_1.

To interpret the progressive loss of structure in the ^{3}NH yield spectra when direct dissociation on S_1 via channel (3) becomes important, we postulate that the structure in the ^{3}NH yield spectrum is determined mainly by the time scale for ISC. In the FC region, the N–C coordinate on S_1 is reached near its inner turning point, and thus initially the N–C bond is compressed compared to its equilibrium separation on S_1. The T_1 geometry in the FC region is rather similar,[16] and thus it is reasonable to assume that there is favorable FC overlap between the inner turning points of the nearly isoenergetic vibronic levels in S_1 and T_1. Below the channel (3) threshold, S_1 excitation survives for many vibrational periods, and every time the excited complex samples the inner turning point region, ISC can occur. Thus, the ^{3}NH yield spectrum shows fairly narrow features. In contrast, when the dissociation pathway to ^{1}NH+CO on S_1 is open, the return to the inner turning point region along the N–C coordinate is prevented, and thus the time allotted for ISC is correspondingly shortened. In this situation the ^{3}NH yield spectrum will exhibit a loss of structure. Moreover, it may become even less structured than the corresponding ^{1}NH yield spectrum, if the latter reflects the complete time evolution to channel (3) products on S_1. As discussed above, $S_1 \leftarrow S_0$ excitation accesses a region on the S_1 PES which is repulsive along the N–C coordinate and has a strong gradient in the NCO angular coordinate. While the former propels the system towards dissociation via channel (3), the latter leads to a complicated nuclear motion on S_1 en route to dissociation, probably accounting for the structure in the ^{1}NH yield spectrum. Note that less favorable FC overlap is expected between S_1 and T_1 vibronic levels at large N–C separations, because the T_1 surface is dissociative at all energies above the S_1 origin, and thus unbound in the N–C coordinate.

At excitation energies below the opening of channel (3), H+NCO is the dominant dissociation pathway with a quantum yield $>$0.9.[11] The ^{1}NH+CO yield near its threshold is very low; for example, at 230 nm [$\sim$700 cm^{-1} above $D_0(^1\text{NH+CO})$] it amounts to only $\sim$0.03 of the spin-

allowed dissociation.[7] At the same wavelength, we obtain a ^{1}NH/^{3}NH population ratio of 0.2; i.e., the ^{3}NH quantum yield is 0.10–0.15, indicating that ISC is significant relative to the other intramolecular interactions. The increase in the ^{1}NH/^{3}NH population ratio to $\approx$2 for dissociation at around 225 nm is attributed mainly to the increase in the yield of channel (3), which eventually becomes the dominant dissociation pathway.[2,3,11] The difference between the population ratios measured on the peak and in the valley of the ^{1}NH yield spectrum around 225 nm again indicates a subtle dependence of the competition between dissociation pathways on the nuclear motions excited on S_1. We note that the 230–225 nm region coincides with the inferred onset of direct S_1 participation in the dissociation via channel (3), and is also the region where state-specific behavior and a loss of structure is observed in the ^{3}NH yield spectrum.

In summary, the results reported in this Communication show the competitiveness of the spin-forbidden dissociation over a broad range of excitation energies. We suggest that the loss of structure in the ^{3}NH yield spectrum, when direct dissociation via channel (3) on S_1 is open, reflects the relative change in the time scale of ISC. The exact location of the seam of singlet-triplet intersection as well as the relative roles of direct and indirect spin-orbit couplings await clarification. A qualitatively similar picture, with its characteristic time scales for IC, may also account for the partial loss of structure in the NCO yield spectrum. The existence of three competitive dissociation pathways at wavelengths $<$230 nm opens the way not only to studies of bond-selective dissociation, as reported by Crim and co-workers,[7] but also to detailed examination of promoting modes for IC and ISC, identified via one-photon and IR/UV excitation schemes. Such studies will provide insights into the origin of the observed bond-selectivity and will aid in designing experiments aimed at controlling branching ratios by affecting the relative efficiency of IC, ISC and direct dissociation.

ACKNOWLEDGMENTS

We thank R. Schinke and H.-R. Volpp for communicating results prior to publication. We benefited greatly from discussions with F. F. Crim, R. Schinke, K. Morokuma, S. S. Brown, A. Sanov and C. Wittig. Support by the U.S. Army Research Office and the National Science Foundation is gratefully acknowledged.

[1] R. N. Dixon and G. H. Kirby, Trans. Faraday Soc. **64**, 2002 (1968).
[2] (a) T. A. Spiglanin, R. A. Perry, and D. W. Chandler, J. Phys. Chem. **90**, 6184 (1986); (b) T. A. Spiglanin and D. W. Chandler, J. Chem. Phys. **87**, 1577 (1987); (c) **87**, 1568 (1987).
[3] W. K. Yi and R. Bersohn, Chem. Phys. Lett. **206**, 365 (1993).
[4] B. Bohn and F. Stuhl, J. Phys. Chem. **97**, 4891 (1993).
[5] B. Ruscic and J. Berkowitz, J. Chem. Phys. **100**, 4498 (1994).
[6] J. Zhang, M. Dulligan, and C. Wittig, J. Phys. Chem. **99**, 7446 (1995).
[7] S. S. Brown, R. B. Metz, H. L. Berghout, and F. F. Crim, J. Chem. Phys. **105**, 6293 (1996).
[8] (a) S. S. Brown, R. B. Metz, H. L. Berghout, and F. F. Crim, J. Phys. Chem. **100**, 7948 (1996); (b) S. S. Brown, H. L. Berghout, and F. F. Crim, J. Chem. Phys. **105**, 8103 (1996).
[9] M. Zyrianov, A. Sanov, T. Droz-Georget, and H. Reisler, J. Chem. Phys. **105**, 8111 (1996).
[10] (a) A. Sanov, T. Droz-Georget, M. Zyrianov, and H. Reisler, J. Chem. Phys. (in press); (b) Ber. Bunsenges. Phys. Chem. (submitted).
[11] (a) R. A. Brownsword, T. Laurent, R. K. Vatsa, H.-R. Volpp, and J. Wolfrum, Chem. Phys. Lett. **249**, 162 (1996); (b) **258**, 164 (1996).
[12] A. M. Mebel, A. Luna, M. C. Lin, and K. Morokuma, J. Chem. Phys. **105**, 6439 (1996).
[13] M. Zyrianov, A. Sazonov, R. A. Beaudet, and H. Reisler (unpublished).
[14] A. Ogai, C. X. W. Qian, and H. Reisler, J. Chem. Phys. **93**, 1107 (1990).
[15] C. R. Brazier, R. S. Ram, and P. F. Bernath, J. Mol. Spectr. **120**, 381 (1986).
[16] W.-H. Fang, X.-Z. You, and Z. Yin, Chem. Phys. Lett. **238**, 236 (1995).
[17] R. Schinke, J. Klossika, H. Floethmann, and K. Yamashita (unpublished).